 <b>Arbeitsnotiz</b>	<b>Nr.:</b> SIS04075.HF
<b>Machine Development Experiments on Cavity Synchronization in the SIS12/18</b>	<b>Name:</b> O. Chorniy, H. Damerau, G. Schreiber, B. Zipfel
<b>Verteiler:</b> Bär, Balß, Barth, Blell, Boine, Breitenberger, Chorniy, Damerau, Dolinski, Eickhoff, Forck, Franchetti, Franczak, Gröning, Hülsmann, Hutter, Kaspar, Kirk, Klingbeil, Kumm, König, Laier, P. Moritz, Peters, Redelbach, Reich, Richter, Scheeler, Schreiber, Schütt, Spiller, Steck, Vinzenz, Wilms, Zipfel, Sekretariate Azzara, Ditter	

## Contents

<b>1</b>	<b>Introduction</b>	<b>1</b>
<b>2</b>	<b>Longitudinal beam parameters at injection to the SIS12/18</b>	<b>1</b>
<b>3</b>	<b>Observation techniques</b>	<b>3</b>
3.1	DSP phase measurement . . . . .	3
3.2	Longitudinal bunch spectrogram plots . . . . .	3
<b>4</b>	<b>Observation of the RF capture</b>	<b>4</b>
4.1	Particle losses during the start of acceleration . . . . .	5
4.2	Comparison of phase and time domain measurements . . . . .	5
4.3	Adjustment of the RF capture frequency . . . . .	6
<b>5</b>	<b>Operation with two synchronized RF cavities</b>	<b>8</b>
5.1	Capturing the beam with one or two RF cavities . . . . .	8
5.2	Counter-phase operation of the two RF units . . . . .	10
5.3	Double harmonic tests . . . . .	11
<b>6</b>	<b>Conclusion</b>	<b>12</b>

## Document history

Version	Date	Authors	Remarks
0.50	15/06/2005	H. Damerau B. Zipfel	First preliminary version
0.51	12/07/2005	H. Damerau	Several corrections according to comments from H. Klingbeil

# Machine Development Experiments on Cavity Synchronization in the SIS12/18

O. Chorniy, H. Damerau, G. Schreiber, B. Zipfel

4 July 2005

## 1 Introduction

Machine development (MD) experiments devoted to the longitudinal beam behaviour during the RF capture in the SIS12/18 and simultaneous operation of both RF cavities have been performed during the first beam time of 2005. While the MDs during April and May were parasitic experiments getting limited resources of the accelerator, typically one virtual machine per minute, the synchrotron was available on a primary user basis during one shift between 7th and 8th of June. The main goals of the experiments can be summarized as follows:

- Test and first commissioning of new measurement equipment, i.e. relative phase measurement between the phase of the cavity gap voltage and the bunch phase based on a DSP system as well as direct observation of the particle bunches in time domain by online generation of spectrograms.
- Direct comparison of the common single cavity operation with two synchronized cavities. Both cavities are then acting with the same total voltage on the beam as a single one. This experiment shows the influence of the DSP based cavity synchronization loop.
- Detailed investigation of problems due to the cavity synchronization loop and test of possible counter-measures, including counter-phase operation of the two cavities.

After a short overview of the longitudinal beam parameters during the MDs, a brief introduction to the new measurement techniques is given. The results of the various experiments and their interpretation are presented thereafter. It can be shown that the cavity synchronization is harmful to the beam when both RF cavities are switched on simultaneously instead of sequentially during RF capture. In case of simultaneous ramping, unwanted longitudinal emittance dilution of the bunches occurs because both cavities have an arbitrary phase relationship as long as the control loop thresholds are not reached.

## 2 Longitudinal beam parameters at injection to the SIS12/18

The longitudinal beam quality has been verified by Schottky measurements of the coasting beam at injection flat-bottom before and during every experiment. The Sony-Tektronix 3066 fast spectrum analyzer has been used for this purpose as its measurement speed is by far superior to standard swept spectrum analyzers normally used for Schottky measurements in the SIS12/18. A flat-bottom after injection of some 50 ms is sufficient to collect the data with

the required resolution during just one machine cycle. The raw spectra as delivered from the analyzer are presented in Fig. 1. As expected, the averaged data can be fitted reasonably well with a simple Gaussian function. The conversion to linear power scaling, averaging and

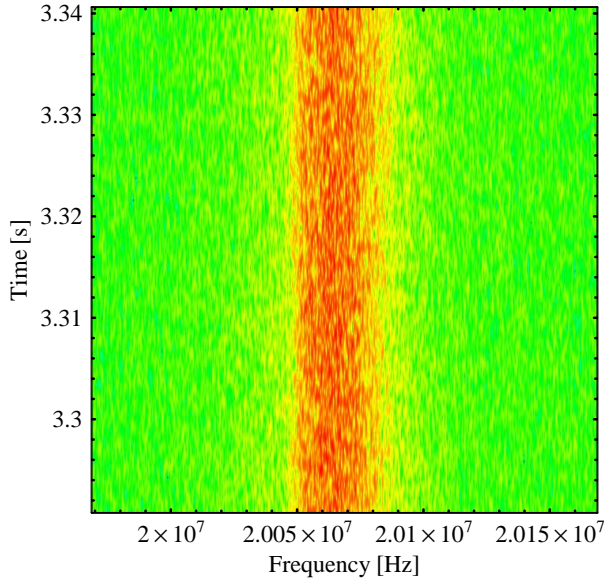


**Fig. 1:** Longitudinal Schottky measurement of a  $^{181}\text{Ta}^{61+}$  in the SIS12/18 at injection flat-bottom taken with the Sony-Tektronix 3066 fast spectrum analyzer during 50 ms injection flat-bottom at the 96th harmonic of the revolution frequency. The color scale corresponds to logarithmic power units, corresponding to the representation on the screen of the instrument itself.

fitting thus finally leads to Fig. 2. The Schottky measurements during the MDs do not show,

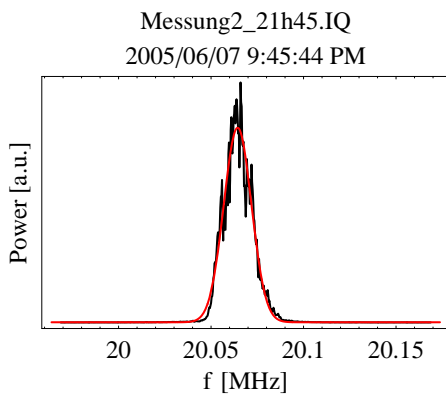


**Fig. 2:** Averaged representation of the raw data shown in Fig. 1 (black curve) and Gaussian fit to the data. At injection energy ( $\gamma \simeq 1$ ) the relative momentum spread corresponds directly to the frequency spread of the distribution, namely  $\Delta p/p|_{2\sigma} \simeq \Delta f/f|_{2\sigma} = \pm 0.8 \cdot 10^{-3}$ .

within the precision limitations due to the averaging and fitting procedure, systematic drifts of the revolution frequency in the SIS12/18 after injection nor a variation of the momentum spread on the timescale of several hours.

If not stated otherwise, the RF frequency during injection, respectively the radial position during injection, adjusted by the so-called RPOSI parameter in the SISModi, was set to the measured revolution frequency of the beam within a precision below  $\pm 100$  Hz ( $\Delta f/f = 1.2 \cdot 10^{-4}$ ). It is worth noting that this precision in tuning the RF frequency is at the achievable limit of the present measurement technique.

The momentum spread of the different kinds of beams used during the different MDs is summarized in Tab. 1. The momentum spread of the injected beam can vary significantly, depending on the ion species. For a beam with a momentum spread as small as  $\Delta p/p|_{2\sigma} \simeq 0.4 \cdot 10^{-3}$  for uranium ( $^{238}\text{U}^{73+}$ ), the adjustment of the RF capture frequency becomes difficult and strong residual longitudinal dipole oscillations could not be avoided.

Date	Ion species	$\Delta p/p _{2\sigma} \simeq \Delta f/f _{2\sigma}$
20/04/2005	$^{86}\text{Kr}^{34+}$	$\pm 1.5 \cdot 10^{-3}$
13/05/2005	$^{238}\text{U}^{73+}$	$\pm 0.4 \cdot 10^{-3}$
07/06/2005	$^{181}\text{Ta}^{61+}$	$\pm 0.8 \cdot 10^{-3}$

**Tab. 1:** Momentum spread of the various beams operated during the MDs.

### 3 Observation techniques

Two observation techniques of the longitudinal beam behaviour recently developed for the SIS12/18, which are now available quasi online, will be briefly introduced in the subsequent paragraphs.

#### 3.1 DSP phase measurement

This measurement technique is a spin-off of the DSP system developed for cavity synchronization and beam phase control [1, 2]. A sketch of the DSP phase measurement system is shown in Fig. 3. The gap signals of either both cavities or the signal of a longitudinal pick can

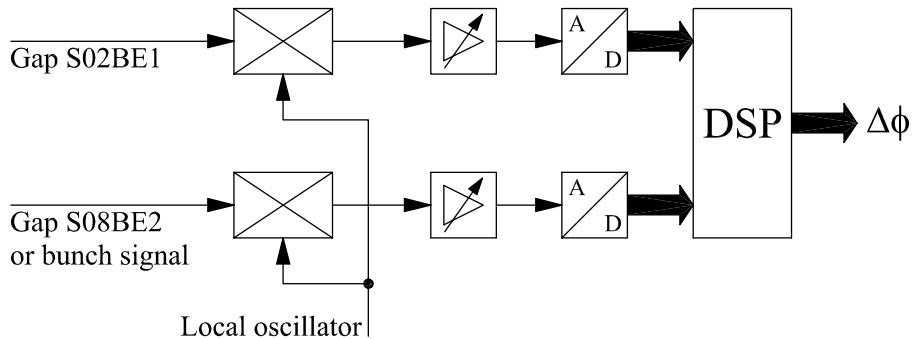


**Fig. 3:** Sketch of the DSP phase measurement system [1].

be used as input signals. After frequency conversion of the swept frequency signal to a fixed intermediate frequency (IF) and amplification, both signals are digitized and fed to a DSP unit which calculates the phase between both signals numerically. It is important to point out that the digitization of all signals takes place at fixed frequency (IF). Furthermore, the DSP system performs narrow band detection which guarantees the proper phase measurement even for noisy signals. A detailed description can be found in [1]. The accuracy of the phase detected by the DSP measurement system is better than  $\pm 1^\circ$  [2].

A typical example of a phase measurement between the gap voltage of the accelerating cavity and the bunch phase during a SIS12/18 cycle is illustrated in Fig. 4.

#### 3.2 Longitudinal bunch spectrogram plots

The complementary measurement in time domain, also using a longitudinal pick-up signal, observes the development of the bunches directly. A schematic overview of the new online bunch spectrogram measurement system is presented in Fig. 5. The measurement profits from the segmented memory functionality of modern digital storage oscilloscopes. The LeCroy

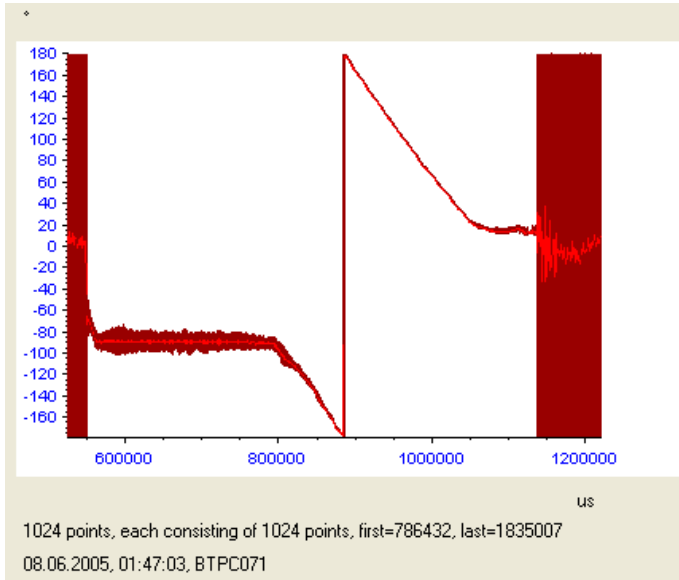


**Fig. 4:** Phase difference between bunch and gap voltage during an acceleration cycle in the SIS12/18 without a phase loop. The light red curve shows the average of the original data (dark red). The areas shaded in dark red are regions before and after the acceleration, where the phase measurement system is fed with noise.

LT374L can record up to 2000 traces, each of which triggered individually. The trigger unit shown in Fig. 5 comprises a (presently fixed) counter being synchronized with the circulating bunches. Every 32 RF periods, corresponding to 8 turns at  $h = 4$  in the SIS12/18, delivered from the DDS reference signal, an output trigger impulse is generated for the oscilloscope to record a short segment of the bunch signal from a longitudinal pick-up. Not only the bunch signal but also cavity gap voltage or the DDS reference signal can be recorded. Additionally, the length of the trigger pulse from the trigger unit corresponds to the RF period and can be used to reconstruct the RF frequency during the measurement.

There are two main advantages of the triggered technique to generate spectrogram plots compared to just recording a single long high-resolution trace: firstly, as data is recorded only every  $n$ th turn, the total amount of recorded data is well below the length of a single high-resolution trace where a large fraction of the recorded data must be filtered and dumped later. This leads to rather short processing times and enables fast online generation of spectrogram plots. Secondly, as all segments are triggered separately and synchronously to the DDS signal being synchronous to the circulating bunches, the time between subsequent segments is correct by definition. If only a single large trace of recorded data is available, the RF frequency is needed later to cut useful segments from the trace and represent them as a spectrogram or waterfall plot.

A flexible set of tools has been programmed in Mathematica [3] to read the data from the oscilloscope via GPIB and LAN, present them as a spectrogram plot and perform more sophisticated computations if necessary. A detailed description of the implementation will be given elsewhere.

A typical spectrogram plot of bunches performing coherent dipole oscillations with the synchrotron frequency is presented in Fig. 6.

## 4 Observation of the RF capture

Both observation techniques introduced above, DSP based phase measurements as well as spectrogram plots, have been used to examine the longitudinal behaviour of the bunches during the RF capture and the start of the acceleration in the SIS12/18. During the start

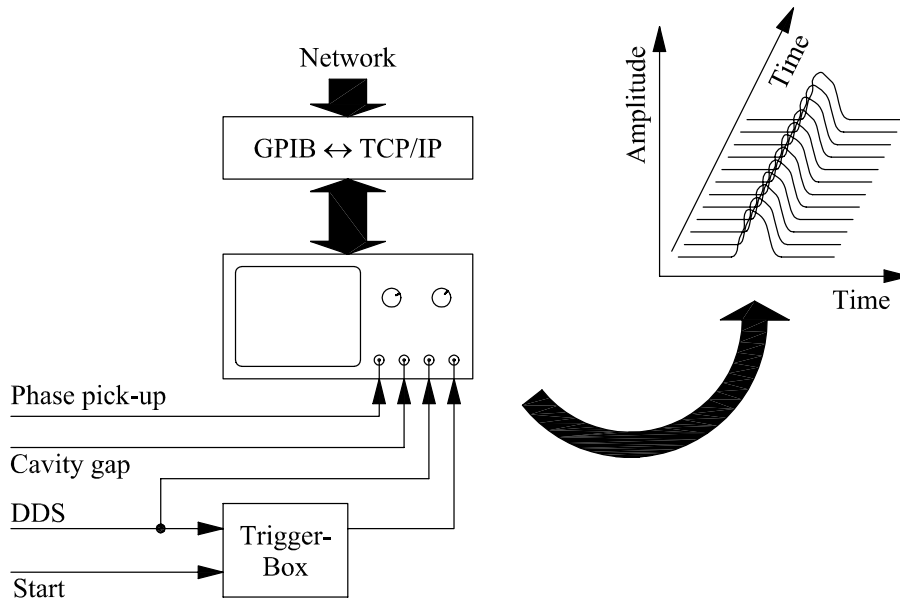


Fig. 5: Sketch of the bunch spectrogram plot measurement system.

of the acceleration, a loss of 5 to 20% of the beam intensity is detected. The loss depends directly on the adjustment of the proper capture frequency, and also the ion species. Similar measurements have already been made in 2002 [4].

#### 4.1 Particle losses during the start of acceleration

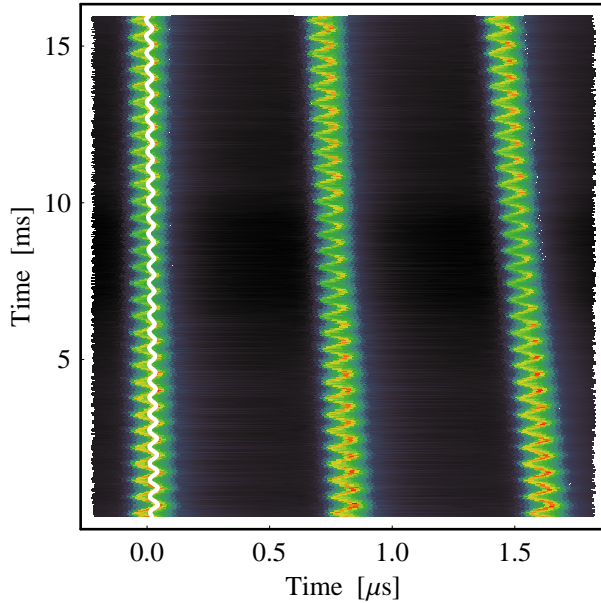
During the MDs in April, the capture efficiency has been systematically measured versus capture frequency. It can be determined easily by comparing the beam intensity measured with the DT\_ML transformer before and after the start of the RF frequency ramp. The capture frequency can be varied independently using the RPOSI parameter in the SISModi.

Fig. 7 shows a typical result of such a frequency sweep. The optimum capture frequency is calculated from a Gaussian fit. However, it should be kept in mind that the capture efficiency only starts to shrink significantly if the frequency deviation is in the range of some 200 Hz. Therefore, other methods to determine the optimum RF frequency, like longitudinal Schottky measurements as well as bunch spectrograms during capture, deliver much better precision than the minimization of the capture losses.

#### 4.2 Comparison of phase and time domain measurements

Depending on whether the beam is bunched at the correct integer harmonic of the revolution frequency of the center of gravity of its energy distribution, a clean RF capture can be observed at least for the  $^{86}\text{Kr}^{34+}$  beam.

An example for a clean RF capture recorded with the DSP phase measurement system and also with the direct time-domain measurement is illustrated in Figs. 8 and 9. The phase oscillation between bunch and bucket has an amplitude of only a few degrees. This behaviour is confirmed by the spectrogram plot (Fig. 9). The dipole oscillation of the bunches during RF capture is almost negligible.



**Fig. 6:** Coherent dipole oscillation of the bunches in the SIS12/18 during acceleration as an example of a spectrogram plot. The color scale reaches from black (low line density) to red (large line density). The horizontal axis represents the time scale during a fraction of a turn, whereas the vertical timescale comprises several periods of the synchrotron frequency.

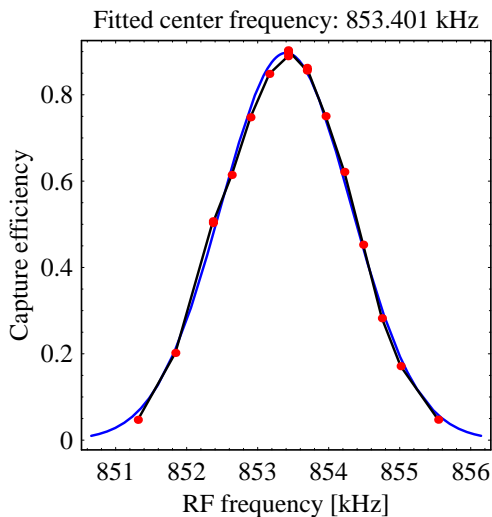


**Fig. 7:** Capture efficiency versus RF frequency during RF capture. As the measurements seem to follow a Gaussian function, a fit was made showing that the optimum RF frequency turns out to be  $f_{\text{RF}} = 853.401$  kHz.

This changes dramatically if the RF frequency is detuned by 530 Hz (Figs. 10 and 11). The bunches oscillate in phase with an amplitude of up to  $45^\circ$  and the strong dipole motion of the bunch core is also visible in spectrogram plot. Unfortunately, the bunch intensities during the experiments in April have been moderate so that the spectrogram plots are perturbed by 50 Hz noise from the mains. Even after numerical filtering, the dynamic range of the measurement (the digitizing oscilloscope has a resolution of eight bits and sometimes the amplitude of the 50 Hz was larger than the bunch signal) is reduced and leads to rather noisy images (Figs. 9 and 11).

### 4.3 Adjustment of the RF capture frequency

Depending on the momentum spread of the beam at injection flat-bottom in the SIS12/18, a clean RF capture, without a significant dipole oscillation of the bunch core, can be achieved by systematic adjustment of the RF frequency to the integer harmonic of the revolution frequency computed from a longitudinal Schottky measurement. This can be easily proven by

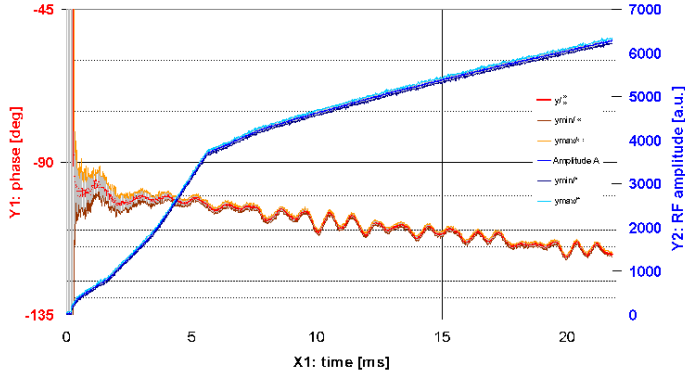


**Fig. 8:** Phase during capture with a well matched RF frequency.

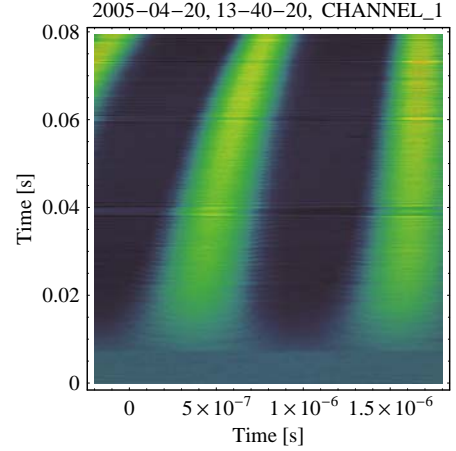


**Fig. 9:** Direct bunch measurement during a good capture.

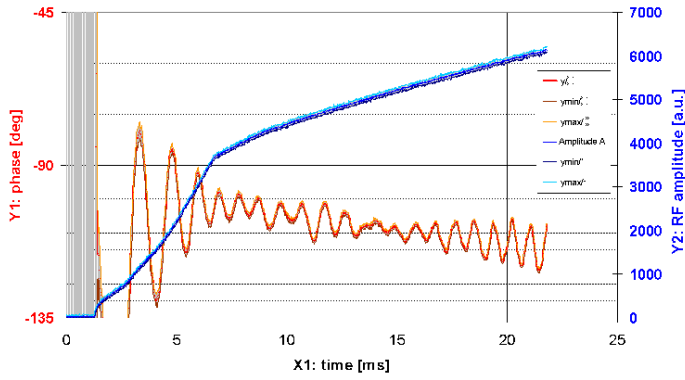


**Fig. 10:** Phase during capture with a strongly mismatched RF frequency ( $\Delta f_{\text{RF}} = 530$  Hz).

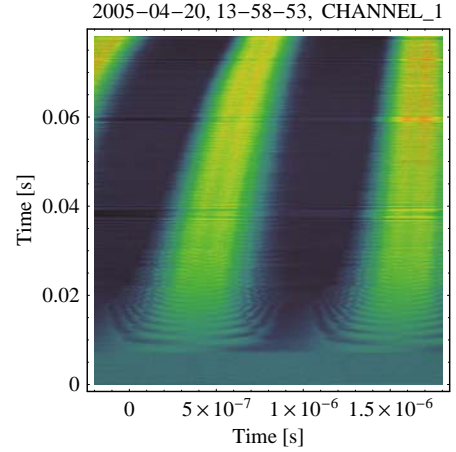


**Fig. 11:** Direct bunch measurement during an mismatched RF capture ( $\Delta f_{\text{RF}} = 530$  Hz).

a longitudinal spectrogram plot, as shown in Fig. 9.

However, for beams with a momentum spread below  $\Delta p/p \simeq \pm 1 \cdot 10^{-3}$ , e.g. the uranium beam as available during the MD in May, it turned out to be impossible to suppress the coherent dipole motion of the bunch core during RF capture. Even after systematic optimization by observing the phase motion of the bunches with the DSP system and the time resolved development of their shape by spectrogram plots, the coherent dipole mode has been present.

It is suspected that the RF capture cannot be adjusted by optimizing the RF parameters alone and that transverse problems during the start of the acceleration potentially contribute to the longitudinal emittance blow observed due to the dipole motion of the bunches. Further experiments are necessary to identify the source of these oscillations.

## 5 Operation with two synchronized RF cavities

During first parasitic beam tests in 2004 with the DSP cavity synchronization [1], it could be shown that the operation of both RF cavities in the SIS12/18 has no negative influence on the accelerated beam intensity. However, no information of the beam quality nor coherent oscillations have been recorded during these first beam tests. A second MD on the comparison of the operation with one or two cavities has been performed in May of this year.

### 5.1 Capturing the beam with one or two RF cavities

When two cavity operation is selected in the SISModi, the given RF amplitude is automatically redistributed to both RF cavities so that, theoretically, no difference between one or two cavity operation should be visible for the beam. Consistent with the results of the measurements in 2004, the beam current transformer does not reveal information whether the RF voltage acting on the beam is generated by one or two cavities. Therefore, the RF capture has been observed in detail.

The dependence of the total RF amplitude generated by two cavities with a given phase deviation is sketched in Fig. 12. When both cavities are operated in phase, the effective sum

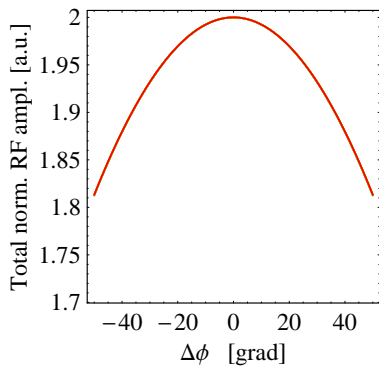


**Fig. 12:** Effective RF voltage generated by two RF cavities versus phase deviation from in-phase operation as reference.

voltage is insensitive against phase errors as well as relative errors of the amplitude loops of the cavities. The accuracy of the cavity synchronization is in the range of few degrees only and thus no limitation is expected due to the residual phase errors between the cavities.

A direct comparison of a the beam behaviour during RF capture using one and two RF cavities generating the same total RF amplitude is illustrated in Figs. 13 and 14. It can clearly be seen, that the coherent dipole oscillations of the bunch core during RF capture are much stronger, when the RF amplitude is generated by two synchronized cavities than by one cavity alone. The reason for this unexpected behaviour could not been figured out during the first MD in May.

Thereafter, this effect was examined in more detail during the MD in June. Amongst different other experiments both, the beam signal and the gap voltage signal have been recorded simultaneously to investigate the phenomenon as can be seen in Figs. 15 and 16. At about 5 ms after the start of the RF capture, a phase jump by almost  $180^{\circ}$  degrees of the gap voltage of the cavity with the regulated DDS is observed (marked as a thick red line in Figs. 15 and 16). Almost exactly at this instant, the start of the coherent dipole oscillations of the bunches is measured with the longitudinal pick-up (see Fig. 16).

The fast phase variation of the two gap signals against each other can also be measured directly with the DSP phase measurement system. Fig. 17 shows the relative phase between

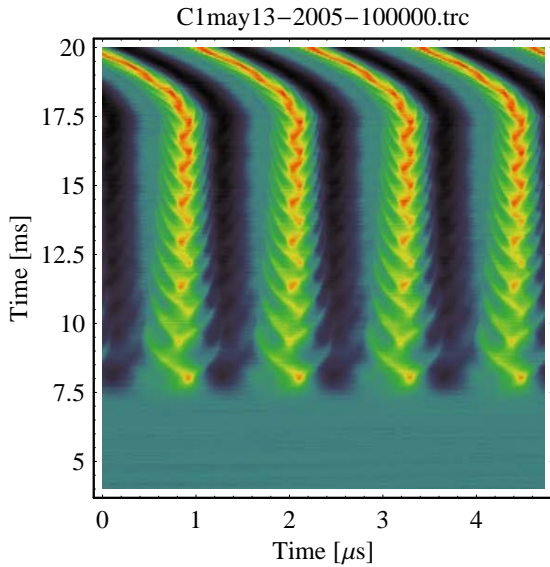


**Fig. 13:** Spectrogram plot of RF capture and start of acceleration using an RF amplitude of 10 kV generated by a single RF cavity (standard mode of operation).

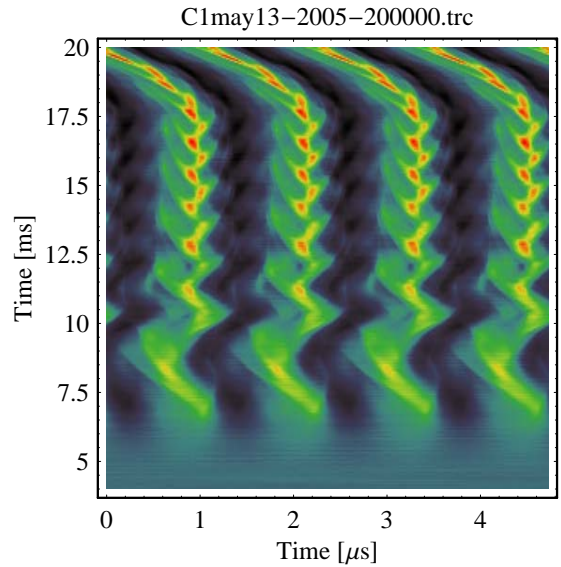


**Fig. 14:** Spectrogram plot of RF capture and start of acceleration as in Fig. 13, but operating both RF cavities with 5 kV synchronized by the DSP electronics.

the cavities during the first few milliseconds of the RF capture. The phase jump is supposed to cause a rapid change in effective phase and amplitude of the two RF cavities seen by the beam.

The mechanism, which finally leads to the dilution of the longitudinal emittance in synchronized two cavity operation, compared to the much better situation for acceleration with a single RF cavity, can be described as follows:

Using one RF cavity, the amplitude and the ferrite tuning loops are the only regulation systems to act on the cavity and therefore on the beam. The threshold of these loops is in the range of some 100 to 200 V. The situation is different when two cavities are operated simultaneously and synchronized with the DSP system. As the DSP electronics synchronizes the gap voltages, a proper phase relationship between both cavities cannot be provided before the gap voltage of each cavity is sufficiently large. This is the case if the amplitude and tuning loops of both cavities work properly, at an amplitude above their threshold of again above 100 to 200 V each, i.e. in the worst case around 400 V in total. With this RF voltage acting on the beam, a large fraction of the particles is already bunched and the fast phase variation due to the start of the DSP phase synchronization can thus trigger the coherent dipole oscillations.

It should be pointed out, that the threshold of the amplitude control loop of each cavity cannot be easily improved or removed. Firstly, the gap voltage of the cavities must cover a large dynamic range which is presently already almost at its limit. Secondly, the possibility to set the RF amplitude to zero in a well defined way is mandatory for the operation modes when a coasting beam is circulating in the SIS12/18; a coasting beam is extremely sensitive against small residual RF voltages. Therefore, a well defined threshold level must be included in the amplitude loops of the cavities. The behaviour of the present amplitude loop during the start of the amplitude ramps is illustrated in Fig. 18. The threshold behavior around an amplitude of 200 V at the gap becomes visible.

Sequential ramping of the RF amplitudes of the two cavities can avoid the threshold

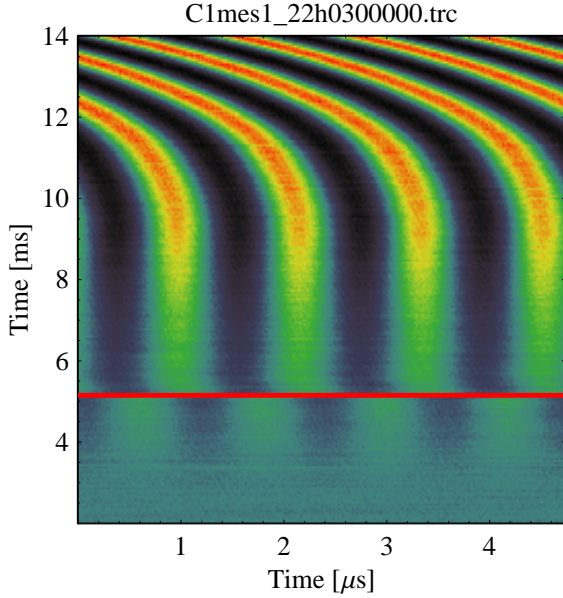


**Fig. 15:** Gap signal of the adjusted cavity during RF capture with both cavities. The red line marks the instant when the phase jump occurs.

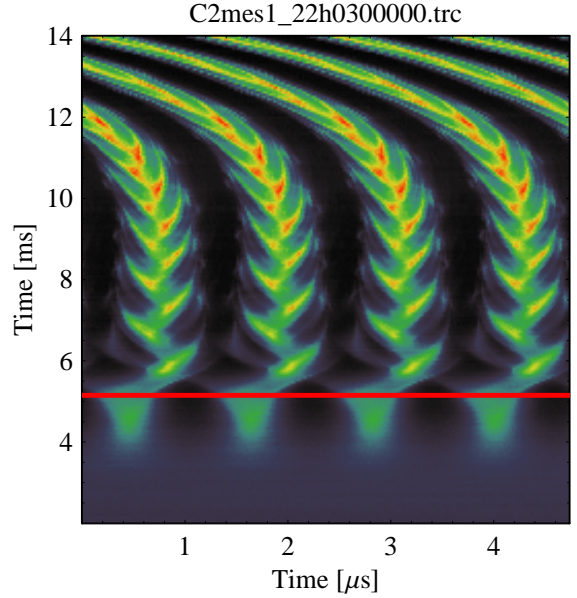


**Fig. 16:** Bunch signal reacting on the sum voltage of the cavity operated from the reference DDS and the gap voltage as shown in Fig. 15.

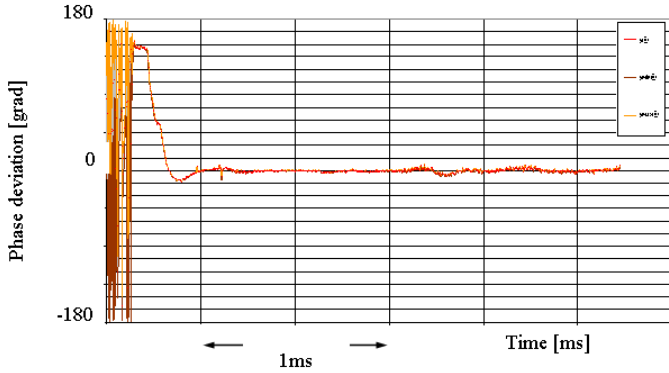


**Fig. 17:** Relative phase between the gap voltages of the two RF cavities. The phase jump at the threshold is clearly visible.

problem. The start of the RF capture, at low voltage, takes place with a single cavity and the second cavity is switched on delayed, when the cavity control loops function reliably.

## 5.2 Counter-phase operation of the two RF units

To check the performance of the DSP phase synchronization, counter-phase operation of both RF units was tried during the MDs. In contrast to in-phase operation, where the total RF amplitude is rather insensitive to relative phase or amplitude errors of the cavities, the residual RF voltage becomes extremely sensitive to these parameters in counter-phase. Equivalent to Fig. 12, the residual effective RF amplitude acting on the beam versus phase error between the two RF cavities is illustrated in Fig. 19. Counter-phase operation allows an independent measurement of the residual RF amplitude acting on the beam, as the synchrotron frequency of the longitudinal dipole mode is proportional to  $U^{1/2}$ , this method is very sensitive to small residual voltages.

Fig. 20 shows an RF capture with both cavities synchronized to a relative phase of  $180^\circ$ .

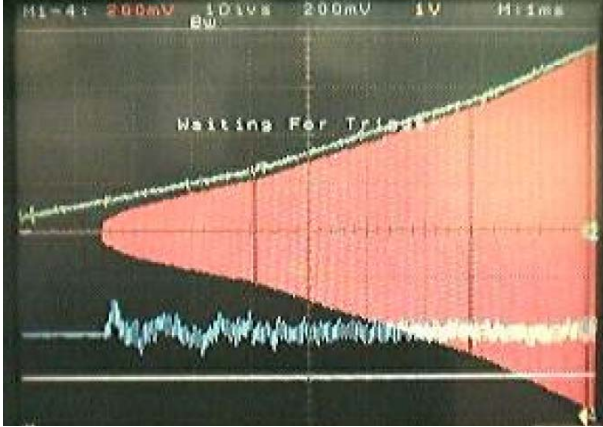


**Fig. 18:** Amplitude reference signal (green) and gap voltage (red) versus time during the RF capture in the SIS12/18. The vertical scaling corresponds to 400 V/div. The blue curve shows the control voltage of the tuning loop.

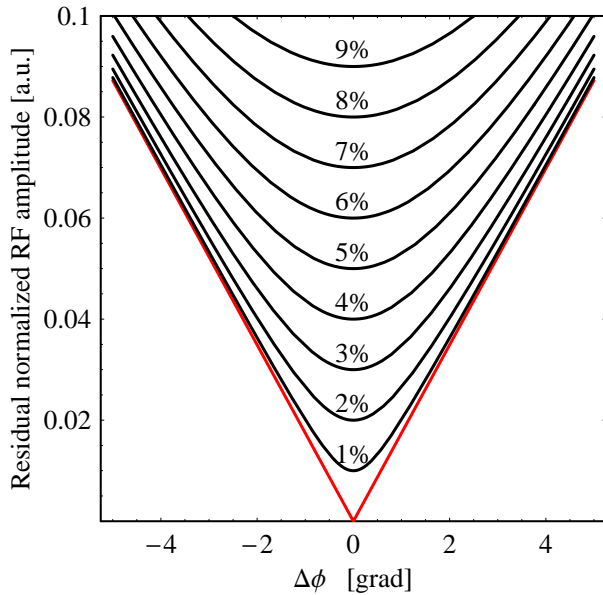


**Fig. 19:** Residual effective RF amplitude generated by two cavities versus phase error (red curve). The black curves give the residual voltage when, due to imperfections of the amplitude loops; a relative amplitude error (given in percent) adds to the phase error.

If the gap voltages of the RF units are perfectly in counter-phase, no bunching should be measurable at all, as the effective RF voltage vanishes theoretically.

However, the formation of bunches is observed and the synchrotron oscillation of the dipole mode reveals that the effective residual RF voltage is about twenty times below the voltage generated by a single cavity. This corresponds, according to Fig. 19, to a phase error below  $4^\circ$ . It was also tried to optimize the relative cavity phase, but no strong dependence of the synchrotron frequency from the phase shift was measured within a range of some  $\pm 8^\circ$ . The residual RF amplitude in counter-phase operation must thus be caused by a combination of phase and amplitude errors. This is consistent with the normally estimated accuracy of the amplitude control loops in the range of 10 to 20 %.

### 5.3 Double harmonic tests

During the last MD, a short test of double harmonic acceleration ( $h = 4$ ,  $h = 8$ ) has been carried out. Due to the upper frequency limitation of the RF systems, the  $^{81}\text{Kr}^{61+}$  beam could only be accelerated to some 120 MeV/u kinetic energy. As the amplitude ramps of the two RF cavities cannot be controlled separately, global scaling parameters available from the

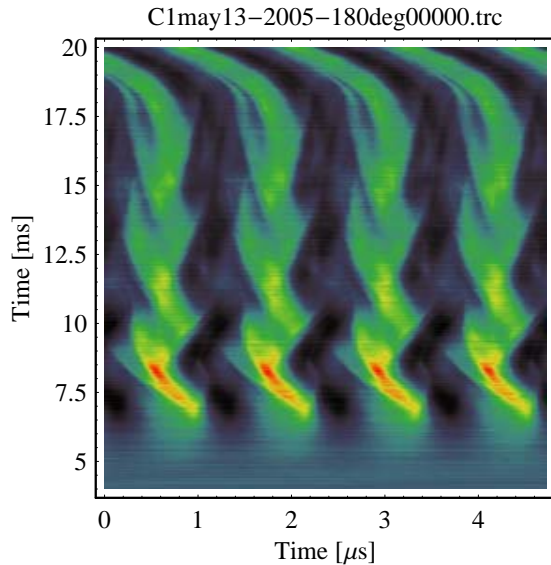


**Fig. 20:** Spectrogram plot of an RF capture with both cavities in counter-phase. The synchrotron frequency of the dipole mode delivers information on the residual RF voltage.

control system have been used. The frequency ramp of S08BE2 has been scaled by a factor of two to set it to  $h = 8$ , while its amplitude ramp has been reduced by a factor of two.

To synchronize both RF cavities based on the DSP phase measurement system according to Fig. 3 at different frequencies, a frequency doubler circuit was inserted into the gap signal of the  $h = 4$  cavity. It is worth noting that the frequency doubler is only an intermediate solution and has a rather limited dynamic range so that a stable synchronization can be only reached at RF amplitudes above several hundred volts per cavity. Furthermore, the same phase jump at the threshold of the synchronization loop, as described in Sec. 5 for two cavities at  $h = 4$ , is observed on the  $h = 8$  cavity. This phase jump again leads to strong longitudinal oscillations of the bunches.

A spectrogram plot taken during the RF capture with two different harmonics  $h = 4$  and  $h = 8$  is shown in Fig. 21, and a single trace of the beam signal from the longitudinal pick-up at about 30 ms is presented in Fig. 22. Despite of the strong oscillations, one can clearly see the bunch lengthening and the double peaked bunch structure due to the higher harmonic RF component at  $h = 4$ . As the phase relationship throughout the acceleration has been kept constant, the symmetric double peak structure vanishes at the start of the frequency ramp. To keep symmetric bunches, the phase must be ramped so that the zero crossing of the higher harmonic RF voltage remains at the synchronous phase.

Due to the failure of the ion source, the MD had to be finished prematurely so that no further test could be made. For further experiments, it would be extremely helpful control the RF cavities with separate frequency and amplitude ramps to optimize the double harmonic acceleration of flat-topped bunches. Additionally a phase ramp (relative phase between  $h = 4$  and  $h = 8$  must delivered to the RF systems to keep symmetrically stretched bunches throughout the cycle.

## 6 Conclusion

Different experiments devoted to the longitudinal beam behaviour in the SIS12/18 have been made during machine development (MD) experiments in April, May and June 2005. Two new online observation techniques, DSP phase measurement and spectrogram plots, could be tested successfully. Their performance is found to be as expected and they have been

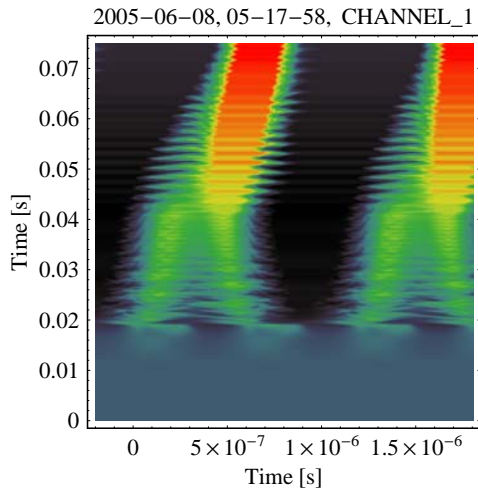


**Fig. 21:** Longitudinal beam signal during double harmonic RF capture ( $h = 4/h = 8$ ). The acceleration begins at about 45 ms after the start of the measurement.

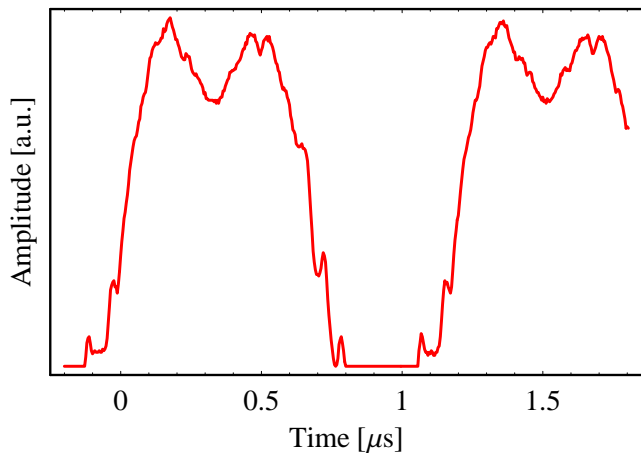


**Fig. 22:** Bunch form as a single trace taken from Fig. 21 at about 30 ms. Unfortunately, the analog to digital converter of the oscilloscope was slightly overloaded.

already proven to be extremely valuable tools during the experiments. Effects could be directly analyzed during the MD, leading to a better understanding of the interaction of the beam with the RF systems.

The minimization of coherent dipole oscillations during injection showed that a nearly clean RF capture is only possible for a coasting beam with a momentum spread above some  $\Delta p/p \simeq \pm 1 \cdot 10^{-3}$ . A coasting beam with a narrow momentum distribution could not be captured without exciting strong dipole oscillations of the bunch core. This behaviour confirms older measurements of the longitudinal emittance taken in 2001. Transverse effects may influence the beam during capture in this case and further investigations are required to identify the source of the coherent dipole motion which is completely unclear for the time being.

The direct comparison between the operation with one or two cavities during RF capture revealed that an RF system consisting of two synchronized cavities has a negative effect on the longitudinal beam quality. This problem has been investigated in detail and it is found that a fast phase jump caused by the synchronization loop triggers the dipole oscillations observed. However, the problem cannot be cured directly as the synchronization loop itself relies on the cavity gap signals which are, by definition, only available at voltages above the threshold of the amplitude loops of the RF systems. Therefore, it is suggested to modify the ramp data for the cavities so that both cavities can be switched on sequentially. Further experiments will show if the effect can be suppressed sufficiently by this technique and also a soft adjustment of the DSP phase synchronization could be considered.

Finally, experiments on counter-phase operation of both cavities have proven the expected precision of the phase synchronization loop and first preliminary tests could be performed on double harmonic acceleration. The improvement of the bunching factor can be shown directly on the bunch profiles at fixed energy.

We would like to thank Martin Kumm for designing and building the electronics of the trigger box used for the spectrogram measurement system.

## References

- [1] H. Klingbeil, *Digitale Kavitätensynchronisation*. GSI internal note, version 1.10, GSI, Darmstadt, 2004
- [2] H. Klingbeil, *A Fast DSP-Based Phase Detector for Closed-Loop RF Control in Synchrotrons*. IEEE Trans. Inst. Meas., Vol. 54, 2005, pp. 1209-1213
- [3] S. Wolfram, *Mathematica: A System for Doing Mathematics by Computer*. Addison-Wesley, Redwood City, California, 1988
- [4] H. Damerau, M. Kirk, Y. Liu, *Maschinenexperimente zum longitudinalen Strahlverhalten während des Hochfrequenzeinfangs*. GSI Arbeitsnotiz SIS28062.HF, GSI, Darmstadt, 2002
- [5] K. Blasche, U. Blell, H. Eickhoff et al., *SIS Status Report*. GSI Report 2000-1, GSI, Darmstadt, pp. 187-188
- [6] H. Damerau, G. Schreiber, P. Spiller, *Maschinenexperimente zur Hochfrequenz-Gymnastik mit zwei Harmonischen (18./19. Dezember 2002)*. GSI Arbeitsnotiz SIS17023.HF, GSI, Darmstadt, 2003